Physics Letters B 690 (2010) 337–345

Contents lists available at ScienceDirect

Physics Letters B

www.elsevier.com/locate/physletb

From model dynamics to oscillating dark energy parameterisation

Aleksandra Kurek [a,*], Orest Hrycyna [b], Marek Szydłowski [a,c]

[a] Astronomical Observatory, Jagiellonian University, Orla 171, 30-244 Kraków, Poland
[b] Department of Theoretical Physics, Faculty of Philosophy, The John Paul II Catholic University of Lublin, Al. Racławickie 14, 20-950 Lublin, Poland
[c] Mark Kac Complex Systems Research Centre, Jagiellonian University, Reymonta 4, 30-059 Kraków, Poland

ARTICLE INFO

Article history:
Received 4 June 2008
Received in revised form 21 May 2010
Accepted 22 May 2010
Available online 27 May 2010
Editor: A. Ringwald

Keywords:
Observational cosmology
Dark energy
Quintessence
Nonminimal coupling

ABSTRACT

We develop here a relatively simple description of dark energy based on the dynamics of non-minimally coupled to gravity phantom scalar field which, in limit, corresponds to cosmological constant. The dark energy equation of state, obtained directly from the dynamics of the model, turns out to be an oscillatory function of the scale factor. This parameterization is compared to other possible dark energy parameterizations, among them, the most popular one, linear in the scale factor. We use the Bayesian framework for model selection and make a comparison in the light of SNIa, CMB shift parameter, BAO A parameter, observational $H(z)$ and growth rate function data. We find that there is evidence to favour a parameterisation with oscillations over a priori assumed linear one.

1. Introduction

The recent discovery of the acceleration of the Universe is one of the most significant discoveries over last decade [1,2]. Observations of distant supernovae type Ia [1,2] as well as cosmic microwave background (CMB) fluctuations [3,4] and large scale structure (LSS) [5] indicate that the Universe is undergoing an accelerating phase of expansion. These observations suggest that the Universe is filled by dark energy of unknown form, violating the strong energy conditions $\rho_X + 3p_X > 0$ or a dynamical equation governing gravity should be modified. A simple cosmological constant model of dark energy can serve the purpose of explanation of dark energy and is in good agreement with the astronomical data (supernovae type Ia and other measurements). Although this model is favoured by the Bayesian framework of model selection [6–9], it faces the serious problem of fine tuning [10]. Therefore the other alternatives [11] have been proposed which includes an evolving scalar field. When one tries to accommodate a time-varying equation of state, the simplest parameterisation is the one which adds a linear dependence on the scale factor a. Other choices are motivated by a possibility of integration dark energy density in an exact form. In this context a class of simple oscillating dark energy equation of state coefficients appeared [12–16]. It is interesting that these models may provide a way to unify the early inflation and the late time acceleration. Moreover in these scenarios we obtain a possible way to solve the cosmic coincidence problem [17–19].

If we allow that the dark energy density might vary in time (or redshift) then there appears a problem of choosing or finding an appropriate form of parameterisation of the equation of a state parameter $w_X(z)$. In the most popular approach $w_X(z) = p_X/\rho_X$ appears to be virtual and the dynamical dark energy parameterisation makes the model phenomenological, containing free parameters and functions. As a result we have a model difficult to constrain [20]. Another approach is to postulate a quintessence potential of the scalar field which has motivation from fundamental physics (particle physics) and then extracts it from the true dynamics directly [21–24]. In this approach we can expect that the parameterisation of dark energy equation of state reflects some realistic underlying of the physical model. The most popular dynamical form of dark energy offers the idea of quintessence. In this conception dark energy is described in terms of the minimally coupled to gravity scalar field ϕ with the potential $V(\phi)$. The scalar field is rolling down its potential starts to dominate the energy density of the standard matter [25,26]. The oscillating scalar field as a quintessence model for dark energy has been recently proposed [27–29]. The case of extended quintessence introduced by Amendola [30] was also considered in our previous papers [21–23] where we assumed the non-zero coupling constant. The possibility of violating of the weak energy condition (phantom scalar field) was admitted. In this scenario, instead of standard minimally coupled scalar field, the phantom scalar field, non-minimally coupled to

* Corresponding author.
E-mail addresses: kurek@oa.uj.edu.pl (A. Kurek), hrycyna@kul.lublin.pl (O. Hrycyna), hrycyna@kul.lublin.pl (M. Szydłowski).

0370-2693
doi:10.1016/j.physletb.2010.05.061

gravity, causes the accelerating phase of expansion of the Universe [21,22]. We found that in the generic case trajectories are approaching the de Sitter state after an infinite number of damping oscillations around the mysterious $w_X = -1$ value. Therefore the ΛCDM model appears as a global attractor in the phase space (ψ, ψ') (where ψ is a phantom scalar field and $' = \mathrm{d}/\mathrm{d}\ln a$).

In this Letter, we aim at testing and selecting the viability of different parameterisations of oscillating dark energy in the light of recent astronomical data. We focus our attention on the equation of state for a non-minimally coupled to gravity phantom scalar field with the potential in the simple quadratic form.

2. Class of kinessence models

This class of models is understood as a class of FRW models with standard dust matter and dark energy parameterised by redshift, i.e. $w_X = w_X(z)$ [25,26]. For simplicity the flat FRW model ($k = 0$) is assumed. Then dynamics of the model is determined by the acceleration equation

$$\frac{\ddot{a}}{a} = -\frac{1}{6}\big(\rho_{\mathrm{m}} + (1+3w_X)\rho_X\big) = -\frac{1}{2}H^2\big(\Omega_{\mathrm{m}} + (1+3w_X)\Omega_X\big), \tag{1}$$

where a is the scale factor, dot is a differentiation with respect to the cosmological time, Ω_{m} and Ω_X are density parameters for matter and dark energy X, respectively, $H = (\ln a)^{\cdot}$ is the Hubble parameter.

We assume that standard matter with energy density $\rho_{\mathrm{m}} = \rho_{\mathrm{m},0}a^{-3}$ is a dust matter and energy density of the dark energy is given, from conservation condition, by $\rho_X = \rho_{X,0}a^{-3}\exp[-3\int_1^a \frac{w_X(a')}{a'}\,\mathrm{d}a']$.

The acceleration equation (1) admits the first integral (which is called Friedman's first integral) in the form

$$\left(\frac{H}{H_0}\right)^2 = \Omega_{\mathrm{m},0}(1+z)^3 + \Omega_{X,0}f(z), \tag{2}$$

where H_0 and $\Omega_{i,0}$ are parameters referring to the present epoch, and z is the redshift related to the scale factor by the relation $1+z = a^{-1}$ (the present value of the scale factor $a_0 = 1$). The phenomenological properties of dark energy are described in terms of the function $f(z)$ such that $f(z) = \exp[3\int_0^z \frac{1+w_X(z')}{1+z'}\,\mathrm{d}z']$.

In the context of the accelerated expansion of the Universe most theoretical models of dark energy are based on scalar fields. It is a consequence of exploring an analogy to the inflationary theory of the primordial universe [31]. However, a single canonical scalar field cannot explain the range of the coefficient of the equation of state $w < -1$ which is preferred by the astronomical data [8]. One possibility, that has received much attention, is that we formally allow the scalar field to have a negative kinetic energy and switch its sign in comparison with canonical scalar field. There are some physical motivation for introducing such a phantom scalar field arising from string/M theory and in supergravity [32]. Another possibility lies in introduction of the coupling term $\xi R\psi^2$ between the scalar field and the gravity (for the review and references see [33]). Such a theory offers scalar–tensor models of a dark energy called extended quintessence.

If we assume that a source of gravity is the phantom scalar field ψ with an arbitrary coupling constant ξ then the dynamics is governed by the action

$$S = \frac{1}{2}\int \mathrm{d}^4x\sqrt{-g}\big(m_p^2R + \big(g^{\mu\nu}\psi_\mu\psi_\nu + \xi R\psi^2 - 2V(\psi)\big)\big), \tag{3}$$

where $m_p^2 = (8\pi G)^{-1}$ and $V(\psi)$ is a scalar field potential.

The phantom cosmology with general potentials was studied by Faraoni [34] using language of qualitative analysis of differential equation to obtain the late time attractors without the specific assumptions of the shape of potential functions. There are many reasons why we should consider a non-zero coupling constant ξ. First, a non-zero ξ is generated by quantum corrections even if it is absent in the classical action (see [35] and references therein). Another reason is that the non-minimal coupling is motivated by the renormalization of the Einstein–Klein–Gordon equation. Of course the value of the coupling constant should be fixed by the physics only, but in relativity any value of the parameter ξ different from $1/6$ (conformal coupling) gives rise to the violation of the equivalence principle [36].

In our paper [22] we studied generic features of the evolutional paths of the flat FRW model with the phantom scalar field non-minimally coupled to gravity by using dynamical systems methods. We reduced dynamics of the model to the simple case of autonomous dynamical system on the invariant submanifold (ψ, ψ') (a prime denotes differentiation with respect to the natural logarithm of the scale factor)

$$\begin{aligned}
&\psi' = y,\\
&y' = -y - y^2(y+6\xi\psi)\frac{1-6\xi}{1+6\xi\psi^2(1-6\xi)} - \frac{1+(1-6\xi)y^2+6\xi(y+\psi)^2}{1+6\xi\psi^2(1-6\xi)}\left[\frac{2\psi(y+6\xi\psi)-(1+6\xi\psi(y+\psi))}{\psi}\right],
\end{aligned} \tag{4}$$

where $V(\psi) \propto \psi^2$ is assumed, and we found that principally there is one asymptotic state, which corresponds to the critical point in the phase space $\psi_0 = \pm 1/\sqrt{6\xi}$ and $\psi_0' = 0$. This critical point is also the de Sitter state ($w_X = -1$). Note that in this model a problem of the big rip singularity does not appear in contrast to the standard phantom cosmology where it is present because the late time attractors in the phase space represent the de Sitter stage. There are two types of evolutional scenarios leading to this Lambda state (depending on the value of ξ), through

1. the monotonic evolution toward the critical point of a node type for $0 < \xi \leqslant 3/25$ (Fig. 1), in the special case $\xi = 3/25$ we obtain a degenerate node;
2. the damping oscillations around the critical point of a focus type for $3/25 < \xi < 1/3$ (Fig. 2).

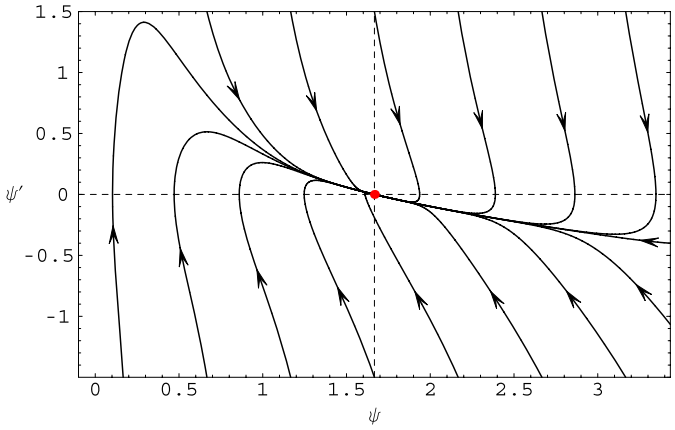

Fig. 1. The phase portrait represents generic behaviour of the system (4) around the critical point of a stable node type.

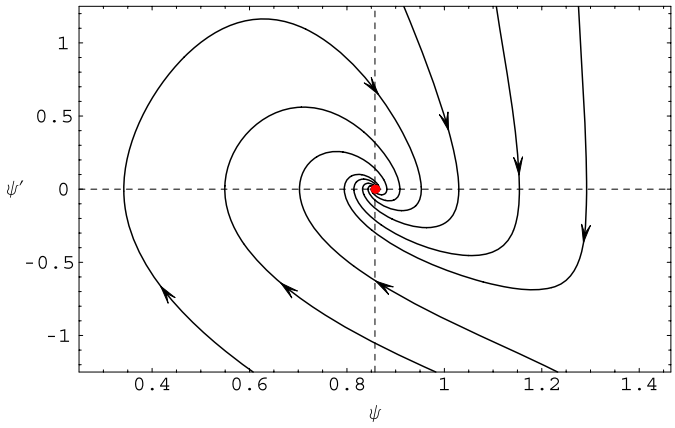

Fig. 2. The phase portrait represents the generic behaviour of the system (4) around a focus type critical point.

The effect of a non-minimal coupling can be treated as an effect of fictitious fluid with some effective coefficient of the equation of state given by

$$w_{\text{eff}} = \frac{2}{1+6\xi\psi^2(1-6\xi)}\left\{\frac{1}{2}\left[1+2\xi\psi^2(1-6\xi)\right]-(1-2\xi)\left[1+(1-6\xi)\psi'^2\right]-4\xi(1-3\xi)\left(\psi'+\psi\right)^2\right\}. \tag{5}$$

In both evolutional scenarios we can find linearised solutions of the dynamical system in the vicinity of the critical point, which the following Hartman–Grobman theorem are good approximations of the system.

Finally one can compute linearised formulas for $w(z)$ around the corresponding critical point for both cases (see Appendix A).

In what follows we concentrate on the special case of parameterisation (A.2) with $\xi = 1/6$ which corresponds to the conformally coupled phantom scalar field [36]. We will confront it (using the Bayesian model selection method) with most popular dark energy parameterisations of $w_X(z)$, which are presented in Table 1.

Recently, it has been argued that models with oscillating dark energy are favoured over a model with a linear parameterisation of EoS [23,17].

3. Results

3.1. Bayesian method of model comparison

To find the best parameterisation of $w_X(z)$ we use the Bayesian method of model comparison [39]. Here the best model (M) from the set of models under consideration is the one which has the greatest value of the probability in the light of the data (D) (posterior probability)

$$P(M|D) = \frac{P(D|M)P(M)}{P(D)}. \tag{6}$$

$P(M)$ is the prior probability for model M, $P(D)$ is the normalisation constant and $P(D|M)$ is the model likelihood (also called evidence) and is given by $P(D|M) = \int P(D|\bar{\theta}, M)P(\bar{\theta}|M)\,\mathrm{d}\bar{\theta}$, where $P(D|\bar{\theta}, M) = \mathrm{L}(\bar{\theta})$ is the likelihood function for model M and $P(\bar{\theta}|M)$ is the prior probability for the model parameters $\bar{\theta}$. It is convenient to consider the ratio of the posterior probabilities for models which we want to compare $\frac{P(M_1|D)}{P(M_2|D)} = \frac{P(D|M_1)}{P(D|M_2)}\frac{P(M_1)}{P(M_2)}$. If we have no prior information to favour one model over another one $(P(M_1) = P(M_2))$, posterior ratio is reduced to the ratio of the model likelihoods, so-called Bayes factor (B_{12}), which values can be interpreted as the strength of

Table 1
Different dark energy parameterisations in terms of $w_X(z) \equiv p_X/\rho_X$ – the coefficient of EoS.

Case	Parameterisation
(1)	Chevallier–Polarski–Linder [37,38] $w_X(z) = w_0 + w_1 \frac{z}{1+z}$
(2)	purely oscillating dark energy a) $w_X(z) = w_0 \cos(\omega_c \ln(1+z))$ b) $w_X(z) = -1 + w_0 \sin(\omega_s \ln(1+z))$
(3)	damping osc. DE a) $w_X(z) = w_0(1+z)^3 \cos(\omega_c \ln(1+z))$ b) $w_X(z) = -1 + w_0(1+z)^3 \sin(\omega_s \ln(1+z))$
(4)	damping osc. DE parameterisation determined directly from the dynamics of phantom scalar field model [22] a) $\xi = \frac{1}{6}$: $w_X(z) = -1 - \frac{4}{3}(1+z)^{3/2}((\cos(\frac{\sqrt{7}}{2}\ln(1+z)) + \frac{5\sqrt{7}}{7}\sin(\frac{\sqrt{7}}{2}\ln(1+z)))x_0$ $+ (\cos(\frac{\sqrt{7}}{2}\ln(1+z)) + \frac{\sqrt{7}}{7}\sin(\frac{\sqrt{7}}{2}\ln(1+z)))y_0)$ $- \frac{2}{3}(1+z)^3((\cos(\frac{\sqrt{7}}{2}\ln(1+z)) + \frac{5\sqrt{7}}{7}\sin(\frac{\sqrt{7}}{2}\ln(1+z)))x_0$ $+ (\cos(\frac{\sqrt{7}}{2}\ln(1+z)) + \frac{\sqrt{7}}{7}\sin(\frac{\sqrt{7}}{2}\ln(1+z)))y_0)^2$ b) $\xi = \frac{1}{6}$, $y_0 = \alpha x_0$: $w_X(z) = -1 - \frac{4}{3}(1+z)^{3/2}((1+\alpha)\cos(\frac{\sqrt{7}}{2}\ln(1+z))$ $+ \frac{\sqrt{7}}{7}(5+\alpha)\sin(\frac{\sqrt{7}}{2}\ln(1+z)))x_0 - \frac{2}{3}(1+z)^3((1+\alpha)\cos(\frac{\sqrt{7}}{2}\ln(1+z))$ $+ \frac{\sqrt{7}}{7}(5+\alpha)\sin(\frac{\sqrt{7}}{2}\ln(1+z)))^2 x_0^2$

evidence to favour model M_1 over model M_2 [40]: $0 < \ln B_{12} < 1$ – 'inconclusive'; $1 < \ln B_{12} < 2.5$ – 'weak'; $2.5 < \ln B_{12} < 5$ – 'moderate'; $\ln B_{12} > 5$ – 'strong'.

The values of Bayesian evidence for models with $w_X(z)$ defined in Table 1 were obtained using a nested sampling algorithm [41], which implementation to the cosmological case is available as a part of the CosmoMC code [42,43], called CosmoNest [44–47]. It was changed for our purpose. We assume flat prior probabilities for the model parameters in the following intervals: $\Omega_{\mathrm{m},0} \in [0,1]$ and $w_0 \in [-2,0]$, $w_1 \in [-3,3]$ (Model 1); $w_0 \in [-2,0]$, $\omega_c \in [0,2]$ (Model 2a and Model 3a); $w_0 \in [-2,2]$, $\omega_s \in [0,2]$ (Model 2b and Model 3b); $x_0 \in [-1,1]$, $y_0 \in [-1,1]$ (Model 4a); $x_0 \in [-1,1]$, $\alpha \in [-3,0]$ (Model 4b). The values of evidence were averaged from the eight runs.

3.2. Analysis with SNIa, CMB R and BAO A data

To compare models gathered in Table 1 we use information coming from the sample of $N_1 = 192$ SNIa data [48], which consists of the ESSENCE sample [49] and a SNIa detected by HST [50]. After suitable calibration SNIa could be treated as standard candles and tests on the assumed cosmology could be done. In this case the likelihood function has the following form

$$\mathcal{L}'_{\mathrm{SN}} \propto \exp\left[-\frac{1}{2}\left(\sum_{i=1}^{N_1} \frac{(\mu_i^{\mathrm{theor}} - \mu_i^{\mathrm{obs}})^2}{\sigma_i^2}\right)\right], \tag{7}$$

where σ_i is known, $\mu_i^{\mathrm{obs}} = m_i - M$ (m_i – apparent magnitude, M – absolute magnitude of SNIa), $\mu_i^{\mathrm{theor}} = 5\log_{10} D_{Li} + \mathcal{M}$, $\mathcal{M} = -5\log_{10} H_0 + 25$ and $D_{Li} = H_0 d_{Li}$, where d_{Li} is the luminosity distance, which (with the assumption that the Universe is spatially flat) is given by $d_{Li} = (1+z_i)c\int_0^{z_i} \frac{\mathrm{d}z'}{H(z')}$ and $H(z)$ is defined in Eq. (2). After an analytical marginalisation over the nuisance parameter $\mathcal{M}$ one can obtain the likelihood function $\mathcal{L}_{\mathrm{SN}}$ which does not depend on the parameter H_0.

We also include information coming from the CMB data using measurement of the shift parameter ($R^{\mathrm{obs}} = 1.70 \pm 0.03$ for $z_{\mathrm{dec}} = 1089$) [4,51], which is related to the first acoustic peak in the temperature power spectrum and is given by $R^{\mathrm{theor}} = \sqrt{\Omega_{\mathrm{m},0}}\int_0^{z_{dec}} \frac{H_0}{H(z)}\,\mathrm{d}z$. Here the likelihood function has the following form

$$\mathcal{L}_R \propto \exp\left[-\frac{(R^{\mathrm{theor}} - R^{\mathrm{obs}})^2}{2\sigma_R^2}\right]. \tag{8}$$

As the third observational data we use the SDSS luminous red galaxies measurement of A parameter ($A^{\mathrm{obs}} = 0.469 \pm 0.017$ for $z_A = 0.35$) [52], which is related to the baryon acoustic oscillations (BAO) peak and defined in the following way $A^{\mathrm{theor}} = \sqrt{\Omega_{\mathrm{m},0}}(\frac{H(z_A)}{H_0})^{-\frac{1}{3}}[\frac{1}{z_A}\int_0^{z_A} \frac{H_0}{H(z)}\,\mathrm{d}z]^{\frac{2}{3}}$. In this case the likelihood function has the following form

$$\mathcal{L}_A \propto \exp\left[-\frac{(A^{\mathrm{theor}} - A^{\mathrm{obs}})^2}{2\sigma_A^2}\right]. \tag{9}$$

The final likelihood function used in analysis is given by $\mathcal{L} = \mathcal{L}_{\mathrm{SN}}\mathcal{L}_R\mathcal{L}_A$.

The results, i.e. values of $\ln B_{1i}$ together with their uncertainties, computed with respect to the model with linear in a parameterisation of $w_X(z)$, are presented in the first column of Table 3.

As we can conclude there is weak evidence to favour model with purely oscillations (2b) over the model with linear in a parameterisation. The comparison with Models 2a, 3b and 4a is inconclusive, which means that the data set used in analysis is not enough powerful

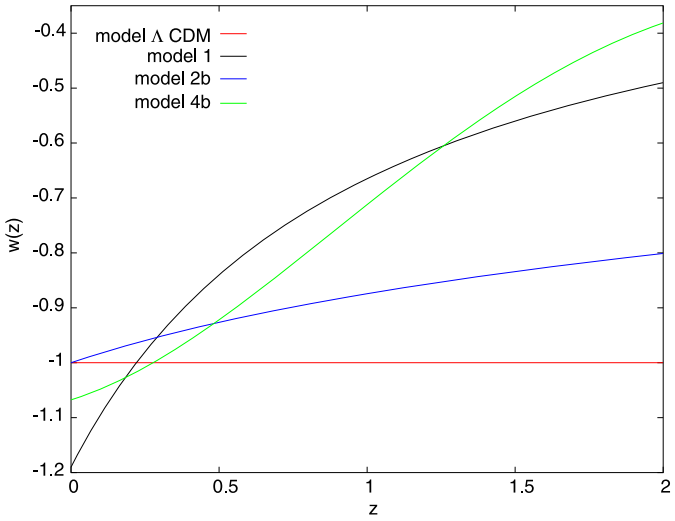

Fig. 3. The functions $w(z)$ for the ΛCDM model, model with linear in a parameterisation of $w(z)$ (1), model with purely oscillations (2b) and model with damping oscillations (4b), calculated for the best fit values of model parameters (SNIa + CMB R + BAO A data).

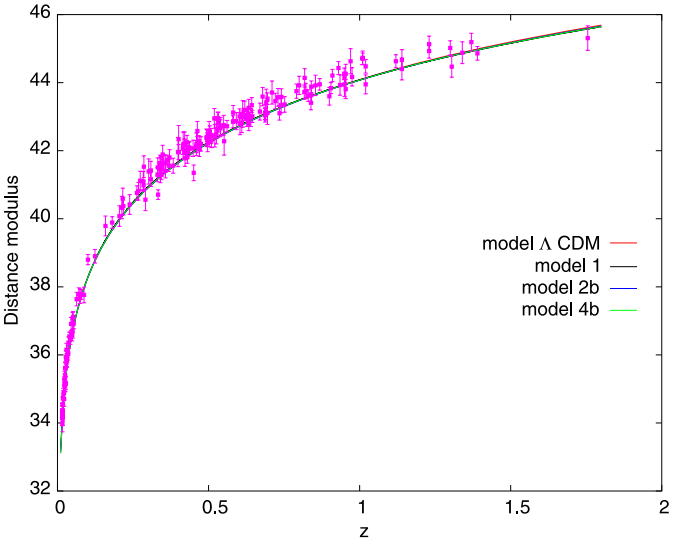

Fig. 4. The distance modulus vs redshift relations for the ΛCDM model, model with linear in a parameterisation of $w(z)$ (1), model with purely oscillations (2b) and model with damping oscillations (4b), calculated for the best fit values of model parameters (SNIa + CMB R + BAO A data) and with the assumption that $H_0 = 72\ \mathrm{km\,s^{-1}\,Mpc^{-1}}$. The SNIa data set is also presented.

to distinguish those models. Additional information coming from different data set or more accurate data set is required. The value of logarithm of the Bayes factor calculated with respect to Model 4b is close to -1, which could indicates on the weak evidence in favour of it, but more information is needed to make the conclusion more robust. There is moderate evidence to favour Model 1 over the model with damping oscillations (3a).

We can also check if the damping term, i.e. $(1+z)^3$, is required by the data. Comparing Model 2a with 3a one can conclude that there is moderate evidence to favour the purely oscillations ($\ln B_{2a3a} = 4.32$), while comparing 2b with 3b that there is weak evidence to favour purely oscillations ($\ln B_{2b3b} = 2.13$).

The comparison of the best parameterisation from the set of models with purely oscillations (2b) over the best one among the models with damping oscillations (4b) does not give conclusive answer: $\ln B_{2b4b} = 1.06$.

Finally one can compare models with dynamical dark energy with parameterisations of the equation of state gathered in Table 1 with the simplest alternative, i.e. the ΛCDM model with $w = -1$. As one can conclude this model is still the best one in the light of SNIa data, CMB R shift parameter and BAO A parameter. However, the conclusion from the comparison of the ΛCDM model with the purely oscillating model (2b) is inconclusive ($\ln B_{\Lambda\mathrm{CDM},2b} = 1.05$).

It is interesting that the model with purely oscillations (2b) is favoured by the data over the model with linear in a parameterisation of $w(z)$. Also the model with damping oscillations (4b) fares well when compared with Model 1. One can try to understand the reason of such conclusions. In Fig. 3 the functions $w(z)$ for the ΛCDM model, Model 1, Model 2b and Model 4b are presented, which were calculated for the best fit values of the model parameters (obtained in the analysis with the SNIa, CMB R and BAO A data). While in Fig. 4 we present the corresponding distance modulus vs redshift relations (with the additional assumption that $H_0 = 72\ \mathrm{km\,s^{-1}\,Mpc^{-1}}$).

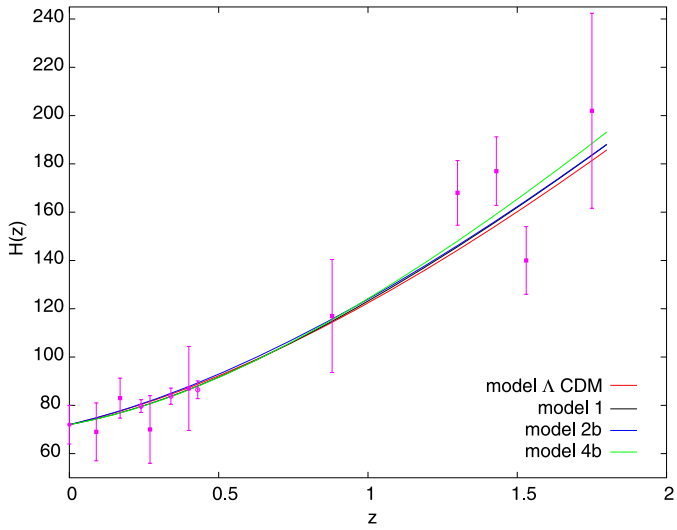

Fig. 5. The $H(z)$ functions for the ΛCDM model, model with linear in a parameterisation of $w(z)$ (1), model with purely oscillations (2b) and model with damping oscillations (4b), calculated for the best fit values of model parameters (SNIa + CMB R + BAO A + H data). The filled square, circle and filled circle points correspond to observational H data from [53–55], respectively.

As we can conclude in spite of the prominent differences in the functions $w(z)$, the distance modulus relations are nearly identical for those models. One should keep in mind that parameters were fitted using the data which are based on the luminosity distance. In this case $w(z)$ is integrated twice.

3.3. Analysis with $H(z)$ data added

It is interesting to consider the relation $H(z)$, as it depends on the $w(z)$ through one integral. Unfortunately, the present Hubble function measurements on different redshifts are small and inaccurate. However, $H(z)$ data set could gives us another insight into the problem considered.

One possibility to measure the Hubble parameter as a function of redshift is based on the differential ages $\mathrm{d}t/\mathrm{d}z$ of passively evolving luminous red galaxies (LRG), which correspond to the Hubble function through the relation

$$H(z) = -\frac{1}{1+z}\frac{\mathrm{d}z}{\mathrm{d}t}. \tag{10}$$

Using Gemini Deep Deep Survey and archival data the authors of [53] obtained nine values of the Hubble parameter for different redshifts in the range $0.09 < z < 1.75$. Although this data set is small and has large uncertainties we include it in our analysis.

Another method to determine the Hubble function values at various redshifts is based on the line of sight (LOS) baryon acoustic oscillation scale measurements. The scale of the BAO in the radial direction depends on the $H(z)$. On the other hand the precise measurement of this scale is given by the CMB observations, so the comparison gives us the value of Hubble parameter. Based on this method and using the SDSS DR6 luminous red galaxies data the authors of [54] obtained the values of H at three different redshifts. The uncertainties are highly reduced when compared with the previous data set. We include those points in our analysis.

To complete our $H(z)$ data set we use the HST measurement of H_0 [55].

We repeat previous calculations with the additional $N_2 = 13$ Hubble function measurements. The corresponding likelihood function has the following form: $\mathcal{L} = \mathcal{L}_{\mathrm{SN}}\mathcal{L}_R\mathcal{L}_A\mathcal{L}_H$, where

$$\mathcal{L}_H \propto \exp\left[-\frac{1}{2}\sum_{i=1}^{N_2}\left(\frac{(H^{\mathrm{theor}}(z_i) - H_i^{\mathrm{obs}})^2}{\sigma_{Hi}^2}\right)\right]. \tag{11}$$

The values of $\ln B_{1i}$ together with uncertainties are gathered in the second column of Table 3. As one can conclude the inclusion of $H(z)$ data does not change our conclusion in most cases. There is still weak evidence to favour of model with purely oscillations (2b) over the model with linear in a parameterisation of w. Evidence in favour of Model 4b becomes slightly greater (weak evidence to favour this model over the Model 1). The evidence against Model 3a is even greater than in previous calculations, we find strong evidence against it.

The evidence to favour model with purely oscillations (2a) over the model with damping term (3a) is strong ($B_{2a3a} = 6.2$), while the evidence in favour of Model 2b over the Model 3b is moderate ($B_{2b3b} = 2.57$).

The comparison of the best model among the models with purely oscillations, i.e. 2b, with the best model from the set of models with damping term, i.e. 4b, does not give the conclusive answer $B_{2b4b} = 0.99$. As one can conclude the ΛCDM model is still the best one from the models considered, however, the conclusion from the comparison with Model 2b is inconclusive ($B_{\Lambda\mathrm{CDM},2b} = 0.97$).

We present the relations $H(z)$ for Model 1, Model 2b, Model 4b and the ΛCDM model in Fig. 5. The Hubble functions were derived for the best fit model parameters in the analysis with SNIa, CMB R, BAO A and observational $H(z)$ data.

As one conclude the relations $H(z)$ for models considered are similar in the redshift range under consideration. More data with better quality is required. The most promising future H data will come from the BAO measurements. This method gives us much more precise data points when compared with the alternative method.

Table 2
The values of distortion parameter β, bias parameter b and corresponding growth rate function $f = \beta b$ which are used in the calculations.

z	β	b	f	References
0.15	0.49 ± 0.09	1.04 ± 0.11	0.51 ± 0.11	[57,58]
0.35	0.31 ± 0.04	2.25 ± 0.08	0.70 ± 0.18	[5]
0.77	0.70 ± 0.26	1.30 ± 0.10	0.91 ± 0.36	[59]
3.00	–	–	1.46 ± 0.29	[60]

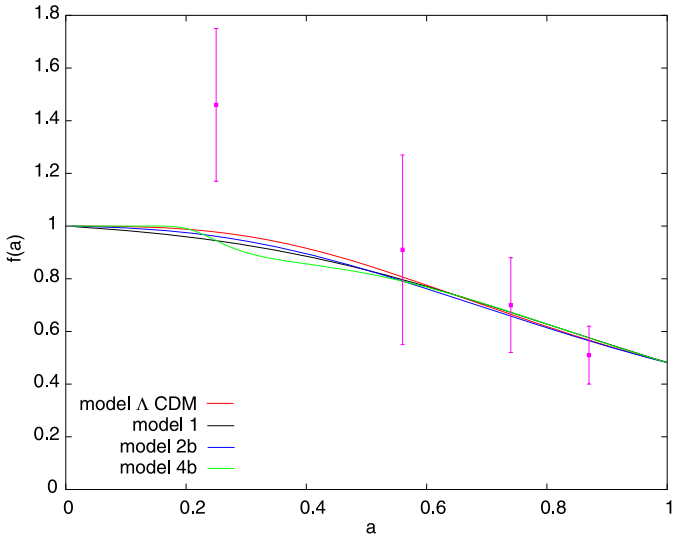

Fig. 6. The $f(z)$ functions for the ΛCDM model, model with linear in a parameterisation of $w(z)$ (1), model with purely oscillations (2b) and model with damping oscillations (4b), calculated for the best fit values of model parameters (SNIa + CMB R + BAO $A + H + f$ data).

3.4. Analysis with growth rate function data added

The conclusions stated before are based on the geometrical dark energy probes. It is interesting to check how the inclusion of the dynamical probes, related to the growth of structures, will change the results. We consider observations of the growth rate function f, which is related to the growth function D by the following formula $f \equiv \mathrm{d}\ln D/\mathrm{d}\ln a$. Its evolution in the general relativity framework is described by the following equation

$$a\frac{\mathrm{d}f}{\mathrm{d}a} = -f^2 - f\left(\frac{1}{2} - \frac{3}{2}\big(1 - \Omega_{\mathrm{m}}(a)\big)w(a)\right) + \frac{3}{2}\Omega_{\mathrm{m}}(a), \tag{12}$$

where $\Omega_{\mathrm{m}}(a) = \frac{\Omega_{\mathrm{m},0}a^{-3}}{H^2/H_0^2}$.

The values of growth rate (f^{theor}) at various scale factor (a) for considered models were obtained with the help of Eq. (12). It was solved using numerical methods, with the assumption that $f(a \simeq 0) = 1$.

The observational growth rate data (f^{obs}) could be obtained through the measurements of the redshift distortion parameter β. It is observed through the anisotropic pattern of galactic redshifts on cluster scales. It is related to the growth rate function by the following formula $\beta \equiv f/b$. The so-called bias parameter b reflects the fact that the galaxy distribution does not perfectly trace the matter distribution in the Universe. Currently there are only few measurements of f available (see Table 2). This data set is similar to the one presented in [56]. We do not consider the data points at $z = 0.55$ and $z = 1.4$, as the bias parameter was derived with the help of the value β in those cases. The measurement at $z = 3$ was obtained in different method, which does not rely on β and b parameters. The value of f is finding in the analysis with Ly-α forest data.

It should be kept in mind that this data set was obtained with the assumption of the ΛCDM model. Its inclusion in the analysis with other models could decrease its reliability and the results should be treated with care.

The likelihood function used in analysis is of the following form $\mathcal{L} = \mathcal{L}_{\mathrm{SN}}\mathcal{L}_R\mathcal{L}_A\mathcal{L}_H\mathcal{L}_f$, where

$$\mathcal{L}_f \propto \exp\left[-\frac{1}{2}\sum_{i=1}^{N_3}\left(\frac{(f^{\mathrm{theor}}(a_i) - f_i^{\mathrm{obs}})^2}{\sigma_{fi}^2}\right)\right], \tag{13}$$

where $N_3 = 4$. The values of $\ln B_{1i}$ and its uncertainties are gathered in the third column of Table 3.

As one can conclude the final conclusions do not change in all cases. The data set is not informative enough to change results.

In Fig. 6 one can find a plot of the growth rate as a function of the scale factor for the ΛCDM model, Model 1, Model 2b and Model 4b, calculated for the best fit values of model parameters (in the analysis with SNIa, CMB R, BAO A, H and f data).

The relation $f(a)$ for model 4b differs from the other relations. Anyway the data points have large uncertainties, which prevent this set to distinguish models considered. This is in agreement with our previous conclusion.

Table 3
The values of $\ln(B_{1i}) = \ln P(D|M_1) - \ln P(D|M_i)$ calculated with respect to the model with linear in a parameterisation of $w_X(z)$ for different data sets.

Model	SNIa + CMB R + BAO A	SNIa + CMB R + BAO $A + H$	SNIa + CMB R + BAO $A + H + f$
1	0	0	0
2a	0.29 ± 0.22	0.33 ± 0.21	0.18 ± 0.22
2b	-2.08 ± 0.13	-2.14 ± 0.20	-2.24 ± 0.23
3a	4.61 ± 0.18	6.53 ± 0.24	6.3 ± 0.23
3b	0.05 ± 0.12	0.43 ± 0.23	0.34 ± 0.25
4a	0.5 ± 0.13	0.31 ± 0.23	0.25 ± 0.24
4b	-1.02 ± 0.18	-1.15 ± 0.23	-1.21 ± 0.23
ΛCDM	-3.13 ± 0.16	-3.11 ± 0.22	-3.3 ± 0.23

3.5. Discussion

In spite of the fact that models with oscillating relation for $w(z)$ (i.e. 2b and 4b) fare well when compared with the model in which $w(a)$ is a linear function of scale factor, the oscillating behaviour is not seen in the $w(z)$ vs z plots in the redshift interval considered. While the frequency parameter of the Model 4b is fixed by the theory, it appears as a free parameter in Model 2b. The relation for $w(z)$ in Model 4b is complicated. However, it can be rewritten as sum of sine and cosine components, with the amplitudes, which depend on z, as well as on the model parameters. On the other hand frequency parameters w_s are equal to $\sqrt{7}/2$ or $\sqrt{7}$. If we consider the relation $|w_s \ln(1+z)| = 2\pi$, we can claim that the oscillating behaviour should be observed in the redshift range of about $\Delta z \simeq 10$. Unfortunately, most of the data points used in analysis are for $z < 2$. The oscillating behaviour is not seen. More observations at higher redshifts are needed. On the contrary, as was stated before, the frequency parameter of Model 2b is a free one. The assumed prior range for this parameter (i.e. $w_s \in [0, 2]$) corresponds to the period of oscillation of at least $\Delta z \simeq 22$. It is again too big to be observed with the present data sets. It is interesting to consider the situation in which the oscillating behaviour could be detected. It can be done by assessing a different prior range for frequency parameter. We repeat calculations for Model 2b, with the assumption that $w_s \in [2, 4.5]$ (Model 2b1). It corresponds to period of oscillations of at least $\Delta z \simeq 3$ (the redshift of the most distant data point, of course apart from the one at $z = 1089$). The value of logarithm of the Bayes factor, calculated with respect to Model 2b, is equal to $\ln B_{2b,2b1} = 4.1 \pm 0.17$. This means that the evidence against Model 2b1 is moderate. We can conclude that available data sets prefer a model with period of oscillations larger than could be detected nowadays.

4. Conclusions

We use the Bayesian method of model selection to compare the FRW models with different functional forms of dynamical dark energy (different parameterisations of the EoS). We examine two categories of parameterisations: a priori assumed and derived from the model dynamics. We show that two parameterisations are favoured over most popular linear with respect to the scale factor.

In particular we obtain following results:

- parameterisation with purely oscillations, i.e. 2b, is the best one among parameterisation considered in this Letter;
- there is weak evidence to favour this parameterisation over the linear in a parameterisation of EoS (this conclusion is based on the SNIa, CMB R and BAO A data sets and does not change after inclusion observational H and f data);
- data sets used in analysis prefer Model 2b in which oscillating behaviour could not be detected nowadays;
- comparison of Model 4b with the linear in a parameterisation of EoS does not give conclusive answer when it is based on SNIa, CMB R and BAO A data, but after the inclusion of H and f data we find the weak evidence in favour of this model;
- the comparison of the ΛCDM model with the model with dark energy parameterised as 2b is inconclusive, a more accurate data set is required to distinguish those models;
- damping term, i.e. $(1+z)^3$, which appears in parameterisations (3) is not supported by the data used in analysis.

In study of cosmological constraints on the form of dark energy the most popular methodology is study of the viability of different parameterisations for the equation of state parameter. They are postulated rather in the a priori forms without connection with true model dynamics. Our approach is different because we claim that if model dynamics is closed then corresponding form of dark energy parameterisation should be forced. It is because we tested the FRW model with dark energy rather than the parameterisation $w(z)$ itself.

Acknowledgements

This work has been supported by the Marie Curie Host Fellowships for the Transfer of Knowledge project COCOS (Contract No. MTKD-CT-2004-517186). The authors also acknowledge cooperation in the project "Particle Physics and Cosmology: The Interface" (Particles–Astrophysics–Cosmology Agreement for scientific collaboration in theoretical research).

Appendix A. Linearised formulas for $w(z)$

Here we present linearised formulas for $w(z)$ around the critical point corresponding to the de Sitter state for monotonic and oscillating evolution toward this point [22]:

$$w_X^{\mathrm{mon}} = \frac{-(1-3\xi) + f_1(\xi,a)a^{-3/2} + f_2(\xi,a)a^{-3}}{(1-3\xi) + 6\xi(1-6\xi)\psi_0(Aa^{\alpha_l} + Ba^{-\alpha_l})a^{-3/2} + 3\xi(1-6\xi)(Aa^{\alpha_l} + Ba^{-\alpha_l})^2 a^{-3}}, \tag{A.1}$$

where $\psi_0^2 = \frac{1}{6\xi}$, $\alpha_l = \frac{\sqrt{3}}{2}\sqrt{\frac{3-25\xi}{1-3\xi}}$, $A = \frac{1}{2}x_0 + \sqrt{3}\sqrt{\frac{1-3\xi}{3-25\xi}}(\frac{1}{2}x_0 + \frac{1}{3}y_0)$, $B = \frac{1}{2}x_0 - \sqrt{3}\sqrt{\frac{1-3\xi}{3-25\xi}}(\frac{1}{2}x_0 + \frac{1}{3}y_0)$, x_0 and y_0 are the initial conditions for ψ and ψ', respectively, and $f_1 = 2\xi\psi_0((3(1-4\xi) - 4\alpha_l(1-3\xi))Aa^{\alpha_l} + (3(1-4\xi) + 4\alpha_l(1-3\xi))Ba^{-\alpha_l})$, $f_2 = (-\frac{3}{4}(3-4\xi) + 15\xi(1-2\xi))(Aa^{\alpha_l} + Ba^{-\alpha_l})^2 + \alpha_l(3(1-4\xi) - 8\xi(1-3\xi))(A^2a^{2\alpha_l} - B^2a^{-2\alpha_l}) - \alpha_l^2(1-4\xi)(Aa^{\alpha_l} - Ba^{-\alpha_l})^2$, and

$$w_X^{\mathrm{osc}} = \frac{-(1-3\xi) + g_1(\xi,a)a^{-3/2} + g_2(\xi,a)a^{-3}}{(1-3\xi) + 6\xi(1-6\xi)\psi_0 h(\xi,a)a^{-3/2} + 3\xi(1-6\xi)h^2(\xi,a)a^{-3}}, \tag{A.2}$$

where $h = x_0\cos(\alpha_{\mathrm{osc}}\ln a) + \frac{3}{\alpha_{\mathrm{osc}}}\sin(\alpha_{\mathrm{osc}}\ln a)(\frac{1}{2}x_0 + \frac{1}{3}y_0)$, $g_1 = 2\xi\psi_0((1-6\xi)h - 4(1-3\xi)((x_0+y_0)\cos(\alpha_{\mathrm{osc}}\ln a) - \alpha_{\mathrm{osc}}x_0\sin(\alpha_{\mathrm{osc}}\ln a) - \frac{3}{2\alpha_{\mathrm{osc}}}\sin(\alpha_{\mathrm{osc}}\ln a)(\frac{1}{2}x_0 + \frac{1}{3}y_0)))$, $g_2 = \xi(1-6\xi)h^2 - (1-2\xi)(1-6\xi)(y_0\cos(\alpha_{\mathrm{osc}}\ln a) - \alpha_{\mathrm{osc}}x_0\sin(\alpha_{\mathrm{osc}}\ln a) - \frac{9}{2\alpha_{\mathrm{osc}}}\sin(\alpha_{\mathrm{osc}}\ln a)(\frac{1}{2}x_0 + \frac{1}{3}y_0))^2 - 4\xi(1-3\xi)((x_0+y_0)\cos(\alpha_{\mathrm{osc}}\ln a) - \alpha_{\mathrm{osc}}x_0\sin(\alpha_{\mathrm{osc}}\ln a) - \frac{3}{2\alpha_{\mathrm{osc}}}\sin(\alpha_{\mathrm{osc}}\ln a)(\frac{1}{2}x_0 + \frac{1}{3}y_0))^2$, where $\alpha_{\mathrm{osc}} = \frac{\sqrt{3}}{2}\sqrt{\frac{25\xi-3}{1-3\xi}}$ and x_0, y_0 and ψ_0 have their usual meaning.

Note that in all cases purely oscillating scenario does not exist.

References

[1] A.G. Riess, et al., Supernova Search Team, Astron. J. 116 (1998) 1009, astro-ph/9805201.
[2] S. Perlmutter, et al., Supernova Cosmology Project, Astrophys. J. 517 (1999) 565, astro-ph/9812133.
[3] C.L. Bennett, et al., WMAP Collaboration, Astrophys. J. Suppl. 148 (2003) 1, astro-ph/0302207.
[4] D.N. Sperge, et al., WMAP Collaboration, Astrophys. J. Suppl. 170 (2007) 377, astro-ph/0603449.
[5] M. Tegmark, et al., SDSS Collaboration, Phys. Rev. D 74 (2006) 123507, astro-ph/0608632.
[6] M. Szydlowski, A. Kurek, A. Krawiec, Phys. Lett. B 642 (2006) 171, astro-ph/0604327.
[7] M. Szydlowski, A. Kurek, AIP Conf. Proc. 861 (2006) 1031, astro-ph/0603538.
[8] A. Kurek, M. Szydlowski, Astrophys. J. 675 (2008) 1, astro-ph/0702484.
[9] A. Kurek, M. Szydlowski, Nuovo Cimento B 122 (2007) 1359, arXiv:0710.2125.
[10] T. Padmanabhan, Phys. Rep. 380 (2003) 235, hep-th/0212290.
[11] S.A. Bludman, Cosmological acceleration: Dark energy or modified gravity?, astro-ph/0605198, 2006.
[12] E.V. Linder, Astropart. Phys. 25 (2006) 167, astro-ph/0511415.
[13] J.-Q. Xia, B. Feng, X.-M. Zhang, Mod. Phys. Lett. A 20 (2005) 2409, astro-ph/0411501.
[14] G. Barenboim, O. Mena, C. Quigg, Phys. Rev. D 71 (2005) 063533, astro-ph/0412010.
[15] W. Zhao, Chin. Phys. 16 (2007) 2830, astro-ph/0604459.
[16] B. Feng, M. Li, Y.-S. Piao, X. Zhang, Phys. Lett. B 634 (2006) 101, astro-ph/0407432.
[17] D. Jain, A. Dev, J.S. Alcaniz, Phys. Lett. B 656 (2007) 15, arXiv:0709.4234.
[18] K. Griest, Phys. Rev. D 66 (2002) 123501, astro-ph/0202052.
[19] S. Dodelson, M. Kaplinghat, E. Stewart, Phys. Rev. Lett. 85 (2000) 5276, astro-ph/0002360.
[20] R. Crittenden, E. Majerotto, F. Piazza, Phys. Rev. Lett. 98 (2007) 251301, astro-ph/0702003.
[21] O. Hrycyna, M. Szydlowski, Phys. Lett. B 651 (2007) 8, arXiv:0704.1651.
[22] O. Hrycyna, M. Szydlowski, Phys. Rev. D 76 (2007) 123510, arXiv:0707.4471.
[23] A. Kurek, O. Hrycyna, M. Szydlowski, Phys. Lett. B 659 (2008) 14, arXiv:0707.0292.
[24] V. Faraoni, Am. J. Phys. 69 (2001) 372, physics/0006030.
[25] B. Ratra, P.J.E. Peebles, Phys. Rev. D 37 (1988) 3406.
[26] C. Wetterich, Nucl. Phys. B 302 (1988) 668.
[27] S. Dutta, R.J. Scherrer, Phys. Rev. D 78 (2008) 083512, arXiv:0805.0763.
[28] M.C. Johnson, M. Kamionkowski, Phys. Rev. D 78 (2008) 063010, arXiv:0805.1748.
[29] J.-a. Gu, Oscillating quintessence, arXiv:0711.3606, 2007.
[30] L. Amendola, Mon. Not. R. Astron. Soc. 312 (2000) 521, astro-ph/9906073.
[31] L.F. Abbott, Nucl. Phys. B 185 (1981) 233.
[32] L. Mersini-Houghton, M. Bastero-Gil, P. Kanti, Phys. Rev. D 64 (2001) 043508, hep-ph/0101210.
[33] V. Faraoni, M.N. Jensen, Class. Quantum Grav. 23 (2006) 3005, gr-qc/0602097.
[34] V. Faraoni, Class. Quantum Grav. 22 (2005) 3235, gr-qc/0506095.
[35] V. Faraoni, Int. J. Theor. Phys. 40 (2001) 2259, hep-th/0009053.
[36] M. Szydlowski, O. Hrycyna, A. Kurek, Phys. Rev. D 77 (2008) 027302, arXiv:0710.0366.
[37] M. Chevallier, D. Polarski, Int. J. Mod. Phys. D 10 (2001) 213, gr-qc/0009008.
[38] E.V. Linder, Phys. Rev. D 70 (2004) 023511, astro-ph/0402503.
[39] H. Jeffreys, Theory of Probability, 3rd ed., Oxford University Press, Oxford, 1961.
[40] R. Trotta, Contemp. Phys. 49 (2008) 71, arXiv:0803.4089.
[41] J. Skilling, http://www.inference.phy.cam.ac.uk/bayesys/.
[42] A. Lewis, http://cosmologist.info/.
[43] A. Lewis, S. Bridle, Phys. Rev. D 66 (2002) 103511, astro-ph/0205436.
[44] P.M.D. Parkinso, A. Liddle, http://astronomy.sussex.ac.uk/~pm52/cosmonest/.
[45] P. Mukherjee, D. Parkinson, A. Liddle, Astrophys. J 638 (2006) L51, astro-ph/0508461.
[46] P. Mukherjee, D. Parkinson, P.S. Corasaniti, A.R. Liddle, M. Kunz, Mon. Not. R. Astron. Soc. 369 (2006) 1725, astro-ph/0512484.
[47] D. Parkinson, P. Mukherjee, A.R. Liddle, Phys. Rev. D 73 (2006) 123523, astro-ph/0605003.
[48] T.M. Davis, et al., Astrophys. J. 666 (2007) 716, astro-ph/0701510.
[49] W.M. Wood-Vasey, et al., ESSENCE Collaboration, Astrophys. J. 666 (2007) 694, astro-ph/0701041.
[50] A.G. Riess, et al., Astrophys. J. 659 (2007) 98, astro-ph/0611572.
[51] Y. Wang, P. Mukherjee, Astrophys. J. 650 (2006) 1, astro-ph/0604051.
[52] D.J. Eisenstein, et al., SDSS Collaboration, Astrophys. J. 633 (2005) 560, astro-ph/0501171.
[53] J. Simon, L. Verde, R. Jimenez, Phys. Rev. D 71 (2005) 123001, astro-ph/0412269.
[54] E. Gaztanaga, A. Cabre, L. Hui, Mon. Not. R. Astron. Soc. 399 (2009) 1663, arXiv:0807.3551.
[55] W.L. Freedman, et al., HST Collaboration, Astrophys. J. 553 (2001) 47, astro-ph/0012376.
[56] H. Wei, Eur. Phys. J. C 60 (2009) 449, arXiv:0809.0057.
[57] E. Hawkins, et al., Mon. Not. R. Astron. Soc. 346 (2003) 78, astro-ph/0212375.
[58] L. Verde, et al., Mon. Not. R. Astron. Soc. 335 (2002) 432, astro-ph/0112161.
[59] L. Guzzo, et al., Nature 451 (2008) 541, arXiv:0802.1944.
[60] P. McDonald, et al., SDSS Collaboration, Astrophys. J. 635 (2005) 761, astro-ph/0407377.